ISBN: 978-3-95450-231-8 ISSN: 2673-5490 doi: 10.18429/JACoW-IPAC2023-MOPA041

BEAM OPTICS UPDATE FOR EIC HSR-IR2*

D. Xu†, J. S. Berg, W. Bergan, D. Holmes, H. Lovelace III, C. Liu,
S. Peggs, G. Robert-Demolaize, E. Wang, BNL, Upton, NY, USA
B. R. Gamage, Jefferson Lab, Newport News, VA, USA

Abstract

The Insertion Region 2 (IR2) will accommodate a Pre-Cooler at injection energy (24 GeV) and a Strong Hadron Cooling (SHC) facility at top energy (100 GeV and 275 GeV) in the Hadron Storage Ring (HSR) of the Electron-Ion Collider (EIC). This paper summarizes the lattice update in HSR-IR2 to meet the requirements from the Pre-cooling and the SHC. The layout has been changed to provide a longer cooling section. It also describes how to enable vertical cooling for the SHC in IR2.

INTRODUCTION

The Electron Ion Collider (EIC) aims to attain a luminosity of $10^{34}\text{cm}^{-2}\text{s}^{-1}$, requiring the use of a flat proton beam to match the electron beam size at the interaction point (IP). The technique of electron cooling is utilized to pre-cool proton bunches at an injection energy of 23.8 GeV [1] to achieve a flat proton beam profile with small emittance. Once pre-cooled, the proton bunches are then accelerated to the collision energy. At the top energy, strong hadron cooling is essential to counteract emittance growth due to intra-beam scattering during long store time. The EIC Conceptual Design Report [2] has selected Coherent electron Cooling (CeC) [3] as the baseline cooling method, primarily due to its high cooling rate on high-energy protons. The HSR-IR2 is designed to accommodate both strong hadron cooling and pre-cooling.

Figure 1 illustrates a schematic representation of the cooling facility and the HSR-IR2 layout [4]. The strong hadron cooling and the pre-cooling share the same Energy Recovery Linac (ERL). In the case of strong hadron cooling, The protons and electrons co-propagate in the modulator and kicker sections. The Coulomb interaction between protons and electrons in the modulator section results in microscopic energy perturbations on electrons. These perturbations are then amplified in the dispersive chicane section after modulation. The protons also traverse a dispersive section. Following this, the two beams are merged again in the kicker section, where the electric field of the density fluctuations induced in the electron beam acts back on the protons.

This paper will present the lattice design for the HSR-IR2. The HSR-IR2 geometry has been updated to fulfill the prerequisites of strong hadron cooling and pre-cooling. The beam optics are matched for strong hadron cooling at 100 GeV and 275 GeV.

* Work supported by Brookhaven Science Associates, LLC under Contract No. DE-SC0012704 with the U.S. Department of Energy
† dxu@bnl.gov

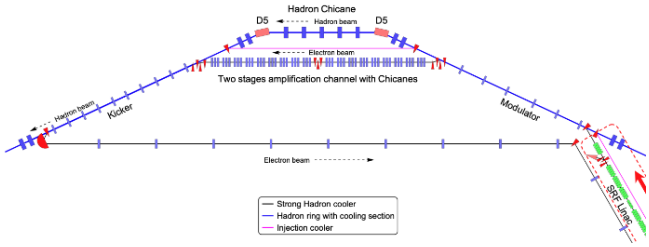

Figure 1: The strong hadron cooler and the pre-cooler in HSR-IR2 share the same Energy Recovery Linac (ERL). Protons co-propagates with electrons in the modulator and kicker sections.

GEOMETRY UPDATE

Figure 2 displays the updated geometry, which has been modified since 2022 [5]. The orbit remains unchanged at the entrance and exit of the HSR-IR2, as depicted in Fig. 3.

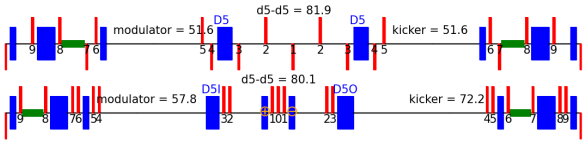

Figure 2: Geometry update of HSR-IR2, top: symmetric, bottom: asymmetric. The quadrupoles are shown as numbered red blocks and the dipoles are indicated by blue blocks. The green blocks have been specifically allocated for the Siberian snakes. The bottom figure shows the revised layout. The symbols ⊕ and ⊖ indicate two dipoles that deflect the orbit in opposite directions.

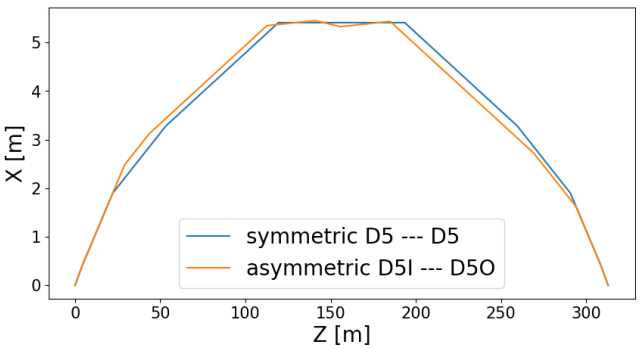

Figure 3: The orbit for old (blue) and new (orange) layout. The entrance and exit of HSR-IR2 stay same as before.

In order to incorporate the Siberian snake into the HSR-IR2, the lattice structure has been altered from a symmetrical to an asymmetrical layout. In the 6-snake arrangement, the

ISBN: 978-3-95450-231-8 ISSN: 2673-5490 doi: 10.18429/JACoW-IPAC2023-MOPA041

snake located in IR2 must be positioned at an exact rotation angle of 180° away from the snake in IR8. However, the snake's location differs between the designs of colliding IR8 and non-colliding IR8. More details about colliding IR8 and non-colliding IR8 can be found in [6]. As a result, the region between Q9 and Q8 on the modulator side, as well as the area between Q6 and Q7, must be reserved for the snake to maintain consistency with IR8. Figure 4 illustrates the 6-snake configuration for both colliding and non-colliding IR8 scenarios. Furthermore, the asymmetric HSR-IR2 design allows for the possibility of reusing the dipoles of D5I and D5O in RHIC.

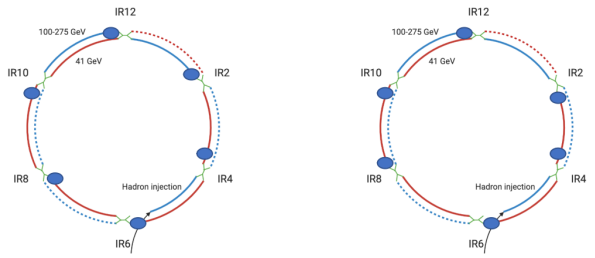

Figure 4: The 6-snake configuration in the HSR, left: non-colliding IR8, right: colliding IR8.

In addition, the total length of the modulator and kicker has been increased from 103 m to 130 m to meet the pre-requisite for pre-cooling. To better match the optics for horizontal cooling, a pair of dipoles has been inserted between the modulator and kicker. In order to maintain the total bending angle, one dipole deflects the orbit inwards, while the other deflects it outwards.

STRONG HADRON COOLING UPDATE

In accordance with the findings presented in [7], under the assumption of a small hadron delay, the cooling rate is proportional to the coefficient denoted by an optical quantity S. In the scenario of an asymmetric HSR-IR2, the S parameter is:

$$S = \frac{D_m D_k}{\sqrt{\beta_m \beta_k}} \left[(\xi_k - \xi_m) \cos\mu + (1 + \xi_m \xi_k) \sin\mu \right] \quad \text{where} \quad \xi \equiv \alpha + \frac{\beta D'}{D}. \tag{1}$$

Here, D and D' represent the momentum dispersion and its slope, respectively. β and α denote the Twiss functions. The subscripts "m" and "k" indicate the quantities defined at the center of the modulator and kicker sections. μ represents the phase advance from the modulator center to the kicker center.

Equation (1) is applicable for both horizontal and vertical planes. In the longitudinal plane, the cooling coefficient is represented by

$$S_z = R_{56}^h - S_x - S_y, \tag{2}$$

where R_{56}^h is the strength of the hadron chicane between the modulator and kicker section. The cooling rates are approximately:

$$(\tau_x^{-1}, \tau_y^{-1}, \tau_z^{-1}) \approx C_\tau (S_x, S_y, S_z), \tag{3}$$

where C_τ is a constant factor.

It is important to keep the delays of the particles small relative to the wake wavelength. According to [8], the typical delay due to the transverse emittance is

$$\Delta Z = \sqrt{2\epsilon T}, \qquad T = \frac{D_m^2}{2\beta_m}\left(1 + \xi_m^2\right) + \frac{D_k^2}{2\beta_k}\left(1 + \xi_k^2\right) + \frac{D_m D_k}{\sqrt{\beta_m \beta_k}} \left[(\xi_k - \xi_m) \sin\mu - (1 + \xi_m \xi_k) \cos\mu \right], \tag{4}$$

where ϵ is the emittance in the horizontal or vertical plane, and T is governed by beam optics. The longitudinal delay caused by the momentum spread σ_δ is expressed as

$$\Delta Z_z = (R_{56}^h - S_x - S_y)\sigma_\delta. \tag{5}$$

Ideally, all of these delays, $(\Delta Z_x, \Delta Z_y, \Delta Z_z)$ should be small in comparison to a quarter wake wavelength. In the matching process, if S_x and S_y are set to a specific value, the longitudinal delay will automatically satisfy the constraint, and hence ΔZ_z is not considered in the matching. The requirements for $S_{x,y}$, $\Delta Z_{x,y}$, and R_{56}^h from Strong Hadron Cooling are summarized in Table 1. These parameters are optimized through the cooling code.

Table 1: Constraints for Cooling Coefficients at 100 GeV and 275 GeV

parameter	relation	unit	275 GeV	100 GeV
S_x	=	mm	0.563	2.575
ΔZ_x	≤	μm	0.408	2.649
S_y	=	mm	0.229	1.527
ΔZ_y	≤	μm	0.210	1.705
R_{56}	=	mm	1.263	6.100

In order to achieve the most favorable cooling rate, it is imperative that the dimensions of the proton beam in the overlapping region are comparable to or less than those of the electron beam, which are determined by the design of the ERL. In the course of this alignment, the mean size of the beams is employed as a criterion, which can be expressed mathematically as follows:

$$< \sigma >= \frac{1}{L}\int_0^L \sigma \, \mathrm{d}s = \frac{1}{L}\int_0^L \sqrt{\beta\epsilon + D^2\sigma_\delta^2} \, \mathrm{d}s, \tag{6}$$

where L is the length of the overlap region in the modulator or kicker sections.

Table 2 presents the constraints for the average size of the proton beam in the modulator and kicker section.

ISBN: 978-3-95450-231-8 ISSN: 2673-5490 doi: 10.18429/JACoW-IPAC2023-MOPA041

Table 2: Constraints for Average Beam Sizes at 100 GeV and 275 GeV

parameter	relation	unit	275 GeV	100 GeV
$< \sigma_{x,m} >$	$\lessapprox$	mm	0.9	1.0
$< \sigma_{y,m} >$	$\lessapprox$	mm	0.4	0.3
$< \sigma_{x,k} >$	$\lessapprox$	mm	0.6	1.0
$< \sigma_{y,k} >$	$\lessapprox$	mm	0.2	0.3

There are 19 quadrupoles in the asymmetric layout in Fig. 2. Their strengths are varied to match the cooling requirements listed in Tables 1 and 2. In addition to cooling demands, there are several other lattice design considerations, such as ensuring that the Twiss functions, including dispersion, are matched at the entrance and the exit. The quadrupole strengths must be less than 0.12 m^{-2} at 275 GeV and 0.33 m^{-2} at 100 GeV. To avoid physical aperture issues, the maximum beam size must not exceed $10\sigma < 33$ mm. Finally, it is essential to maintain the same quadrupole polarity at both 275 GeV and 100 GeV, as well as at injection.

To obtain the global minimum, the BlackBoxOptim package [9] within the Julia programming language is employed. The resulting matches are illustrated in Fig. 5. All listed constraints have been satisfactorily met, except for vertical cooling, which requires vertical dispersion.

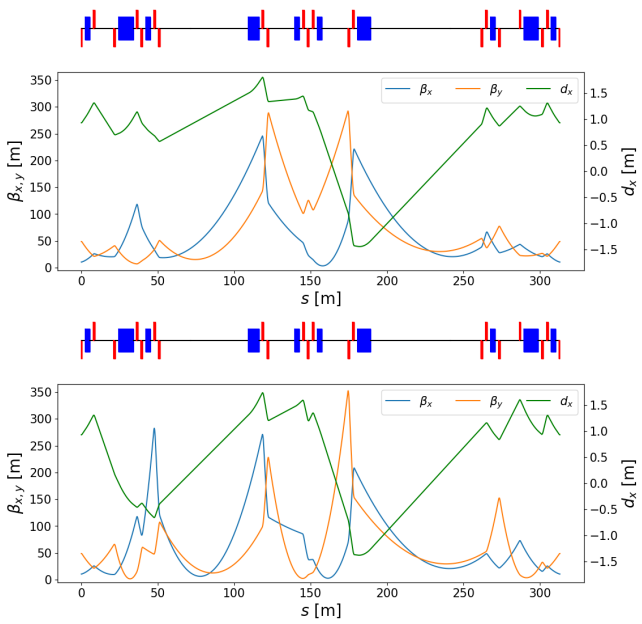

Figure 5: Beam optics matching results, top: 275 GeV, bottom: 100 GeV.

ENABLING VERTICAL COOLING

The vertical dispersion and its slope are normalized as

$$\overline{D} = \frac{D}{\sqrt{\beta}}, \qquad \overline{P} = \frac{\alpha D + \beta D'}{\sqrt{\beta}}. \tag{7}$$

By expressing Eq.(1) in terms of $\overline{D}$ and $\overline{P}$, the cooling coefficient is simplified as

$$S_y = \left(\overline{D}_m \overline{P}_k - \overline{P}_m \overline{D}_k\right) \cos\mu + \left(\overline{D}_m \overline{D}_k + \overline{P}_m \overline{P}_k\right) \sin\mu. \tag{8}$$

If no element is present to create the dispersion between the modulator and kicker centers, the dispersion will undergo a rotation of μ in the normalized space. The rotation is represented as

$$\begin{bmatrix} \overline{D}_k \\ \overline{P}_k \end{bmatrix} = \begin{bmatrix} \cos\mu & \sin\mu \\ -\sin\mu & \cos\mu \end{bmatrix} \begin{bmatrix} \overline{D}_m \\ \overline{P}_m \end{bmatrix}. \tag{9}$$

By substituting Eq. (9) into Eq. (8), the cooling coefficient S becomes zero, indicating that no cooling occurs when no dispersion is generated between the modulator and kicker sections.

To obtain a non-zero value for S_y, two conditions must be met. Firstly, a non-zero vertical dispersion must be present in both the modulator and kicker sections. This can be achieved by using vertical closed orbit correctors of RHIC strength in the two arcs on each side of HSR-IR2 to construct and dampen a local dispersion wave, as described by Peggs [10]. Secondly, a vertical dispersion source between the modulator and kicker sections must be introduced. This can be accomplished by placing skew quadrupoles in the chicane.

The process of optimizing parameters to achieve vertical cooling is currently underway.

SUMMARY

The paper provides an update on the lattice design for the HSR-IR2 in the EIC. The purpose of IR2 is to accommodate a pre-cooler at injection energy and a Strong Hadron Cooling facility at top energy. The original symmetrical layout of IR2 has been transformed into an asymmetrical one to align with the IR8. The lattice design has been updated to meet the requirements of the strong hadron cooling. The method to enable the vertical cooling is discussed.

REFERENCES

[1] A. Fedotov and S. Benson, "Low-energy cooling for the Electron Ion Collider", BNL, Upton, NY, USA, Rep. BNL-220686-2020-TECH, Oct. 2020.

[2] F. Willeke and J. Beebe-Wang *et al.*, "Electron-Ion Collider Conceptual Design Report 2021", BNL, NY, USA, BNL-221006-2021-FORE, 2021. doi:10.2172/1765663

[3] G. Stupakov, "Cooling rate for microbunched electron cooling without amplification", *Phys. Rev. Accel. Beams*, vol. 21, p. 114402, 2018. doi:10.1103/PhysRevAccelBeams.21.114402

[4] E. Wang *et al.*, "Electron Ion Collider Strong Hadron Cooling Injector and ERL", in *Proc. LINAC'22*, Liverpool, UK, Aug.-Sep. 2022, pp. 7–12. doi:10.18429/JACoW-LINAC2022-MO2AA04

[5] S. Peggs *et al.*, "Optics for Strong Hadron Cooling in EIC HSR-IR2", in *Proc. IPAC'22*, Bangkok, Thailand, Jun. 2022, pp. 1920–1923. doi:10.18429/JACoW-IPAC2022-WEPOPT035

ISBN: 978-3-95450-231-8 ISSN: 2673-5490 doi: 10.18429/JACoW-IPAC2023-MOPA041

[6] B. R. Gamage *et al.*, "Second interaction region design concept for the Electron Ion Collider", presented at IPAC'23, Venice, Italy, 2023, paper MOPA022, this conference.

[7] P. Baxevanis and G. Stupakov, "Transverse dynamics considerations for microbunched electron cooling", *Phys. Rev. Accel. Beams*, vol. 22, p. 081003, 2019. doi:10.1103/PhysRevAccelBeams.22.081003

[8] V. Lebedev, "Optical stochastic cooling", *ICFA Beam Dyn. Newslett.*, vol. 65, p. 100, 2014.

[9] https://github.com/robertfeldt/BlackBoxOptim.jl

[10] S. Peggs, unpublished, 2022